

Long-term frequency instability of atomic frequency references based on coherent population trapping and microfabricated vapor cells

Vladislav Gerginov

Department of Physics, University of Notre Dame, Notre Dame, Indiana 46556

Svenja Knappe and Vishal Shah

Department of Physics, University of Colorado, Boulder, Colorado 80309

Peter D. D. Schwindt

Time and Frequency Division, National Institute of Standards and Technology, 325 Broadway M.S. 847, Boulder, Colorado 80305

Leo Hollberg and John Kitching

Time and Frequency Division, National Institute of Standards and Technology, 325 Broadway M.S. 847, Boulder Colorado 80305

Received September 16, 2005; accepted November 17, 2005; posted November 29, 2005 (Doc. ID 64818)

We present an evaluation of the long-term frequency instability and environmental sensitivity of a chip-scale atomic clock based on coherent population trapping, particularly as affected by the light-source subassembly. The long-term frequency stability of this type of device can be dramatically improved by judicious choice of operating parameters of the light-source subassembly. We find that the clock frequency is influenced by the laser-injection current, the laser temperature, and the rf modulation index. The sensitivity of the clock frequency to changes in the laser-injection current or the substrate temperature can be significantly reduced through adjustment of the rf modulation index. This makes the requirements imposed on the laser-temperature stabilization, in order to achieve a given frequency stability, less severe. The clock-frequency instability due to variations in local oscillator power is shown to be reduced through the choice of an appropriate light intensity inside the cell. The importance of these parameters with regard to the long-term stability of such systems is discussed. © 2006 Optical Society of America

OCIS codes: 020.1670, 250.7260.

1. INTRODUCTION

Highly miniaturized chip-scale atomic clocks (CSACs)¹ create possibilities for new practical applications where small size, low power consumption, and good long-term timing stability are required. These atomic clocks are expected to find uses among such other commercially successful timing devices as precision crystal oscillators and compact atomic clocks,²⁻⁴ potentially having the power consumption of the first and the long-term stability of the latter. Physics packages having volumes as small as several cubic millimeters¹ and consuming less than 10 mW of electrical power⁵ have already been demonstrated. Recent table-top experiments have shown that microfabricated vapor cells of millimeter dimensions are capable of supporting frequency instabilities below 5×10^{-12} at 1000 s.⁶ However, when these cells are integrated into a CSAC, the requirement for the small size of the structure makes it potentially much more susceptible to ambient temperature changes owing to the reduced thermal mass of the CSAC, its proportionally large surface area, and the presence of small and highly localized heat sources such as la-

ser or cell heaters. At the same time, the need for low power consumption and small size limits the amount of the precision electronics that can be used to precisely maintain the clock operating parameters at a constant value. In addition, the physics package must be integrated with a local oscillator (LO) having similar size and power dissipation.

There are several aspects that make a CSAC different from a conventional lamp-pumped compact atomic-clock system.⁷ A typical CSAC architecture is shown in Fig. 1(a). First, the light source in a CSAC device is a laser as opposed to a lamp; the wavelength of the laser light depends strongly on the injection current and temperature of the laser. These two dependencies are especially high in vertical-cavity surface-emitting lasers (VCSEIs), which are the lasers of choice in CSAC structures owing to their low power consumption and high modulation efficiency. The change of laser wavelength with temperature and laser injection current makes the clock frequency dependent on laser operating parameters through the AC Stark shift. Second, coherent population trapping (CPT) rather

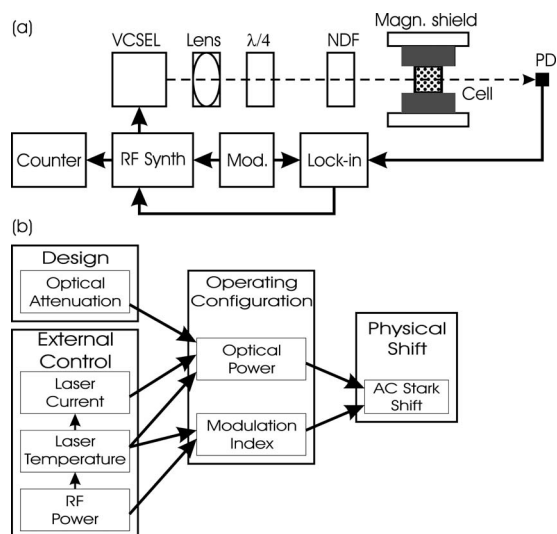


Fig. 1. (a) Experimental setup. VCSEL, vertical-cavity surface-emitting laser; $\lambda/4$, quarter wave plate; NDF, neutral density filter; PD, photodetector. (b) Block diagram showing how the clock design and external controls determine the light field operating configuration and the resulting physical shift of the clock frequency.

than a microwave field is used to excite the hyperfine resonance. The multiplicity of optical field frequencies required for CPT complicate the way in which the AC Stark shift plays a role. If the optical fields are generated by a modulated diode laser, the spectrum depends sensitively on the FM and AM modulation indices. Since the output power of a small, low-power local oscillator is more unstable than that of its counterpart in a compact atomic reference, the dependence of the frequency of the CSAC on the LO output power increases in importance. Therefore, through the AC Stark effect, the external control parameters of the optics assembly (laser current, laser temperature, and RF power) all influence the clock frequency, as shown schematically in Fig. 1(b).

Ambient temperature change is one of the major contributions to the long-term frequency instability of the small clocks. Although the sensitivity of the clock frequency to cell temperature can be largely compensated by use of buffer gas mixtures,^{7,8} the sensitivity of the clock frequency to temperature-induced changes in the parameters of the optics subassembly (which includes the laser) remains an unaddressed difficulty. In this work it is shown that this sensitivity can be significantly reduced. We also show that the sensitivity of the clock frequency to power fluctuations of the local oscillator can be reduced simultaneously, which is important when the size and power consumption of the LO are restricted.

Although this work is intended to improve the performance of a chip-scale device, it is applicable to similar compact atomic clocks based on coherent population trapping.^{4,9}

2. EXPERIMENTAL SETUP

The clock is operated in a conventional, passive coherent-population-trapping configuration, in which the frequency of the local oscillator is locked to a first-order magneti-

cally insensitive CPT resonance excited by a modulated diode laser.^{9,10} A schematic of the experimental setup is shown in Fig. 1(a). A VCSEL, operating in a single longitudinal mode around 795 nm, is used to excite neutral ^{87}Rb atoms confined in a buffer gas cell. The different components of a CSAC assembly are operated together but are spatially separated to allow adjustment of operating parameters and also to uncouple the temperature changes of the laser and the vapor cell. The laser current is modulated at a frequency close to 3.417 GHz, half of the ground-state hyperfine splitting of ^{87}Rb , which generates sidebands on the optical carrier. Pairs of sidebands separated by 6.835 GHz excite a coherent-population-trapping resonance to which the frequency of the rf modulation is locked. The optical power in the first-order sidebands varies between a few percent and 60% as the rf power applied to the laser input port is changed between 8 and 13.5 dBm.

The collimated and circularly polarized laser beam is sent through a neutral density filter (NDF) that controls the beam intensity. After passing through the filter, the beam is sent through the micromachined ^{87}Rb buffer gas cell (interior dimensions $1 \times 1 \times 1$ mm),^{11,12} and the transmitted power is detected with a photodiode placed after the cell. The micromachined cell contains ^{87}Rb and a buffer gas mixture of approximately 6.1 kPa argon and 11.1 kPa neon. The ^{87}Rb optical resonances are homogeneously broadened owing to the presence of the buffer gas in the cell. The linewidth of optical resonances was measured to be 2.2(2) GHz, and the excited-state hyperfine structure is not resolved. The cell is placed inside a cylindrical magnetic shield, and a longitudinal magnetic field of 50×10^{-6} T is applied with a long solenoid mounted inside the shield. A thermistor temperature control is used to keep the cell temperature around 363 K with ~ 1 mK precision. The laser current is tuned so that the optical frequency of each of the first-order sidebands is in resonance with the $F_g=1 \rightarrow F_e=1,2$ and $F_g=2 \rightarrow F_e=1,2$ transitions of the ^{87}Rb D_1 line ($5s\ ^2S_{1/2} \rightarrow 5p\ ^2P_{1/2}$), respectively. The optical absorption of the two first-order sidebands is near 20%.

When the rf is exactly equal to half of the atomic ground-state hyperfine splitting, the laser transmission increases owing to the CPT effect.¹³ The width of the CPT resonance is determined by the ground-state decoherence time, which in turn depends on the intensities of the optical fields. The resonance width in our case is found to be on the order of 1 kHz; the broadening is caused mainly by collisions of the alkali atoms with the cell walls, laser power broadening, and spin-exchange collisions.^{11,14} The ratio of the CPT signal amplitude to the combined optical absorption amplitude of the two first-order sidebands is around 1.5%. To lock the rf to the CPT resonance, the rf synthesizer frequency is modulated at a frequency of 2–3 kHz with an excursion of 2 kHz, and the signal on the photodetector at the modulation frequency is detected with a lock-in amplifier. This error signal is used to steer the frequency of the rf synthesizer, the frequency of which is measured against a more stable frequency reference. The vapor cell buffer gas mixture is chosen to reduce the sensitivity of the $m_F=0 \rightarrow m_F=0$ hyperfine transition frequency to changes in cell temperature.^{7,8} The clock-

frequency shift with temperature for this cell is found to be $4.7 \times 10^{-9} \text{ K}^{-1}$ at a temperature of 363 K.

3. CLOCK FREQUENCY VERSUS LASER-SUBSTRATE TEMPERATURE

The compensation of the AC Stark shift of the clock frequency is a very important issue in CPT clocks. The overall value of the clock frequency is determined by factors such as buffer gas pressure, cell temperature, magnetic field inside the cell, and laser intensity. The buffer gas pressure is largely fixed, the magnetic field can be controlled precisely, and by selecting an optimal mixture of buffer gasses^{7,8} the sensitivity of the clock frequency to changes in cell temperature can be minimized. Choosing an appropriate modulation index of the diode laser can result in cancellation of the total AC Stark shift, making the clock first-order insensitive to the intensity changes inside the cell.^{15–17} This cancellation assumes that the modulation index of the laser optical field is fixed and that the ratio of the amplitude of each sideband in the optical spectrum to the carrier does not change in time.

The laser optical frequency and optical power depend on both the laser substrate temperature (30 GHz/K) and the injection current (150–300 GHz/mA). Therefore, when the diode-laser optical frequency is locked to the Rb absorption resonance through feedback to the laser current, the laser temperature and output power become directly coupled to the laser current. The laser-current adjustment required to maintain a constant optical frequency for a given change in substrate temperature results in a laser intensity change, which causes a variation in the AC Stark shift of the CPT clock frequency. A more subtle effect of a change in the laser temperature at constant optical frequency is that the laser rf impedance^{18,19} and modulation properties^{20,21} are modified, and with them, the distribution of the laser intensity among the carrier and the sidebands because of the different rf coupling. The redistribution of the optical power between the carrier and the sidebands under frequency-locked conditions in turn changes the overall AC Stark shift of the CPT clock frequency. The net result is that the clock frequency depends on the laser substrate temperature in a rather complicated way, which generally means that changes in ambient temperature will contribute to the long-term frequency instability of the clock.

It is well known that because of the α parameter (line-width enhancement factor),^{20,21} the modulation of the injection current produces a combination of AM and FM of the optical field. Also, the ratio of AM to FM indices at a constant modulation frequency varies with temperature owing to changes in the relaxation oscillation frequency. The change of the laser modulation properties with temperature shifts the $m_F=0 \rightarrow m_F=0$ resonance, since the changes in the optical spectrum of the laser lead to a corresponding AC Stark shift of the clock resonance.

In this work, it is shown that it is possible to choose a value for the rf power coupled to the laser such that the AC Stark shift caused by a change in the laser intensity with temperature (owing to a change in the laser current) is compensated by the AC Stark shift associated with the corresponding change in the modulation index, which re-

distributes the optical power between the carrier and the sidebands. The cancellation of the AC Stark shift is illustrated in Fig. 1(b). This cancellation includes the change of the modulation properties of the laser with temperature, in contrast with the method described in Refs. 15–17, in which such parameter change is not considered. Experiments were performed with two types of VCSELs with very different operational parameters—output power, temperature, and injection current. One laser is a bare die chip with an etched mesa structure²² mounted on a substrate at a temperature of 303 K. This laser has a threshold of 1.5 mA, operates at an injection current of 4.6 mA, and generates 1 mW of optical power. The other laser has an oxide-confined structure,²³ is packaged in a TO can, and operates at a temperature of 358 K. It has a threshold of 0.7 mA, operates at an injection current of 1.9 mA, and generates 0.5 mW of optical power. The oxide-confined laser modulates twice as efficiently as the etched mesa laser at low frequencies (300 GHz/mA versus 150 GHz/mA), and its frequency detuning versus temperature is slightly stronger (30 GHz versus 25 GHz). The fractional frequency deviation as a function of the substrate temperature for each laser at different rf power levels is shown in Fig. 2. In Fig. 2(b), the shaded area represents the region where the change in the clock frequency versus laser substrate temperature is minimized. From Fig. 2(a) it is clear that choosing a proper modulation index can make the clock frequency insensitive to changes in laser temperature (and therefore intensity), as previously discussed.^{15,16} Unfortunately, Fig. 2(b) shows that, for some lasers, this reduced sensitivity is achieved only over a limited temperature range.

As an example, the CPT clock was run without actively controlling the temperature of the oxide-confined laser. Two measurements were performed, one with the rf modulation optimized for best CPT amplitude and short-term clock stability, and the other with the rf modulation optimized for reduced clock sensitivity to laser-temperature changes. The results are shown in Fig. 3. It was found that the short-term performance of the clock over the entire range of laser temperatures and rf powers

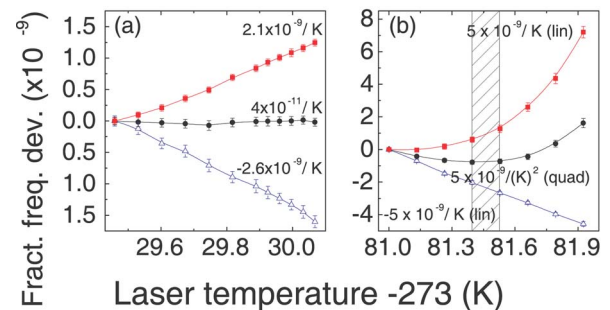


Fig. 2. (Color online) Fractional clock-frequency deviation versus diode laser temperature at different rf powers. (a) Etched mesa laser. Triangles, 11 dBm; circles, 13.5 dBm; squares, 8 dBm. (b) Oxide-confined laser. Triangles, 11 dBm; circles, 9.5 dBm; squares, 8 dBm. The shaded area represents the region where the fractional frequency deviation versus the laser temperature was approximated with a linear (squares, open triangles) or quadratic (circles) dependence. The traces have been offset for convenience. Each point represents 50 s integration time.

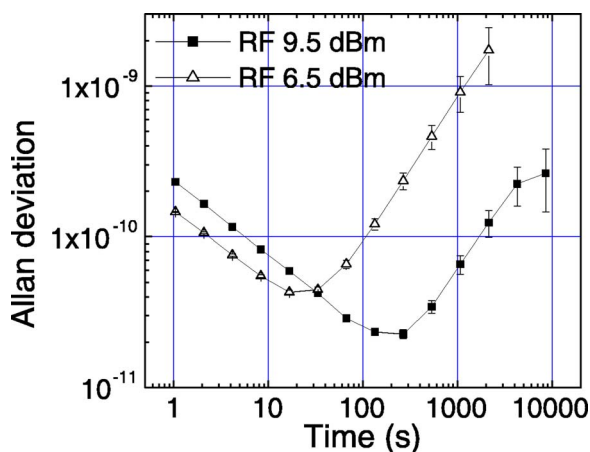


Fig. 3. (Color online) Allan deviation for the CPT clock without laser-temperature compensation (the oxide-confined laser). Triangles, rf power of 6.5 dBm, adjusted for best short-term frequency stability; squares, rf power of 9.5 dBm, adjusted for weakest dependence of clock frequency on substrate temperature.

is unaffected to within a factor of two, indicating that the adjustment of the rf modulation index to the optimal value could be carried out without significantly degrading the clock performance. However, the long-term instability is reduced by more than 1 order of magnitude. Such a reduced sensitivity of the clock frequency to changes in laser temperature was found also at different laser currents and temperatures and is not unique to the parameters shown in Fig. 2.

4. CLOCK FREQUENCY VERSUS rf POWER AT DIFFERENT LASER INTENSITIES

Another important parameter in a chip-scale clock system is the power stability of the local oscillator. If the rf power is used to modulate the laser changes, the laser power will be redistributed between the carrier and sidebands, causing an overall AC Stark shift of the atomic levels and resulting in a frequency change of the CPT clock.^{15,16,24,25} This process is illustrated in Fig. 1(b). The rf power change also alters the laser beam intensity, because the temperature of the diode p-n junction is changed and the frequency lock compensates the temperature change by adjusting the laser injection current. Although the rf power in a commercial rf synthesizer is stable enough that no noticeable drifts of the clock frequency are observed, the situation may be quite different for a compact, low-power local oscillator suitable for integration into a chip-scale device. The CPT clock frequency versus rf power at different light intensities is shown in Fig. 4. As can be seen from the selected region in Fig. 4, it is possible to reduce the drift of the clock frequency caused by rf power changes to $1.4 \times 10^{-12} (\%)^{-2}$ (fractional frequency deviation per rf power change, in percent squared) by choosing an appropriate light intensity inside the cell. The frequency variation (solid triangles) of 7×10^{-10} for a 2 dB change of the rf power around the selected region in Fig. 4 is smaller by a factor of four than the one measured in a similar experiment.²⁵ Again, the short-term stability of the clock is not degraded by more than a factor of two at

any of the light intensities and laser rf modulation levels shown in Fig. 4. The optimization of the clock-frequency dependence on both parameters—laser temperature changes and local oscillator power changes—can therefore be achieved simultaneously, and neither significantly degrades the short-term performance of the clock. When a particular laser temperature and rf power are chosen so that the clock frequency is insensitive to changes in laser temperature, the intensity inside the cell can always be adjusted with the NDF such that the clock frequency becomes simultaneously insensitive to rf power changes. The complex way in which the design and environmental parameters considered here affect the clock frequency is shown in Fig. 1(b).

5. CONCLUSIONS

Although in table-top experiments and under laboratory conditions the laser temperature can be controlled at the millikelvin level and the rf power can be controlled at the level of 0.1%, it is substantially more difficult to attain a similar level of control in a small, low-power device, operating in an environment where the ambient temperature may be changing by tens of kelvins. While the clock frequency drifts due to changes in vapor cell temperature can be compensated by choosing an appropriate buffer gas mixture, the laser intensity change with substrate temperature remains an issue. In this work, it is shown that by properly choosing the laser operating parameters, the clock frequency drifts can be reduced to below the $10 \times 10^{-9} \text{ K}^{-1}$ level. The impact that rf power instabilities have on the clock frequency can also be minimized by adjusting the laser intensity inside the alkali cell. Reducing the small clock sensitivity to these external parameters will lead to a better long-term stability of the clock frequency.

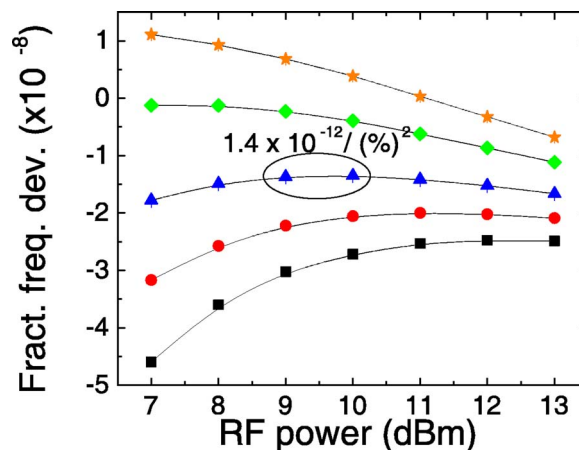


Fig. 4. (Color online) Fractional clock-frequency deviation versus rf power at different laser intensities. Stars, $170 \mu\text{W}/\text{cm}^2$; diamonds, $116 \mu\text{W}/\text{cm}^2$; triangles, $88 \mu\text{W}/\text{cm}^2$; circles, $66 \mu\text{W}/\text{cm}^2$; squares, $53 \mu\text{W}/\text{cm}^2$. The intensity inside the cell was changed by placing a neutral density filter between the laser and the cell. The selected region shows $1.4 \times 10^{-12} (\%)^{-2}$ clock-fractional-frequency deviation per percent squared rf power change. Each point represents 50 s integration time.

ACKNOWLEDGMENTS

The authors thank J. Moreland and L.-A. Liew for the development of microelectromechanical systems (MEMS) processes used in many parts of the structure and the fabrication of MEMS components.

This work was supported by the Microsystems Technology Office of the U.S. Defense Advanced Research Projects Agency. This work is a contribution of the National Institute of Standards and Technology, an agency of the U.S. government, and is not subject to copyright.

V. Gerginov is the corresponding author and can be reached at gerginov@boulder.nist.gov.

REFERENCES

1. S. Knappe, L. Liew, V. Shah, P. D. D. Schwindt, J. Moreland, L. Hollberg, and J. Kitching, "A microfabricated atomic clock," *Appl. Phys. Lett.* **85**, 1460–1462 (2004).
2. M. Bloch, I. Pascaru, C. Stone, and T. McClelland, "Subminiature rubidium frequency standard for commercial applications," in *Proceedings of the 47th IEEE International Frequency Control Symposium* (IEEE, 1993), p. 164.
3. P. J. Chantry, I. Liberman, W. R. Verbanets, C. F. Petronio, R. L. Cather, and W. D. Partlow, "Miniature laser-pumped cesium cell atomic clock oscillator," in *Proceedings of the 50th IEEE International Frequency Control Symposium* (IEEE, 1996), p. 1002.
4. J. Vanier, M. Levine, S. Kendig, D. Janssen, C. Everson, and M. Delaney, "Practical realization of a passive coherent population trapping frequency standard," in *Proceedings of the IEEE International Ultrasonics, Ferroelectrics, and Frequency Control 50th Anniversary Joint Conference* (IEEE, 2004), pp. 92–99.
5. R. Lutwak, J. Deng, W. Riley, M. Varghese, J. Leblanc, G. Tepolt, M. Mescher, D. K. Serkland, K. M. Geib, and G. M. Peake, "The chip-scale atomic clock—low-power physics package," in *Proceedings of the 36th Precise Time and Time Interval (PTTI) Systems and Applications Meeting* (U.S. Naval Observatory, 2004).
6. S. Knappe, V. Gerginov, P. Schwindt, V. Shah, L. Hollberg, and J. Kitching, "Atomic vapor cells for chip-scale atomic clocks with improved long-term frequency stability," *Opt. Lett.* **30**, 2351–2353 (2005).
7. J. Vanier and C. Audoin, *The Quantum Physics of Atomic Frequency Standards*, 1st ed. (Adam Hilger, 1989).
8. W. Happer, "Optical Pumping," *Rev. Mod. Phys.* **44**, 169–249 (1972).
9. J. Vanier, A. Godone, and F. Levi, "Coherent population trapping in cesium: dark lines and coherent microwave emission," *Phys. Rev. A* **58**, 2345–2358 (1998).
10. J. Kitching, S. Knappe, M. Vukicevic, L. Hollberg, R. Wynands, and W. Weidmann, "A microwave frequency reference based on VCSEL-driven dark line resonances in Cs vapor," *IEEE Trans. Instrum. Meas.* **49**, 1313–1317 (2000).
11. L. A. Liew, S. Knappe, J. Moreland, H. Robinson, L. Hollberg, and J. Kitching, "Microfabricated alkali atom vapor cells," *Appl. Phys. Lett.* **84**, 2694–2696 (2004).
12. S. Knappe, V. Velichansky, H. G. Robinson, L. Liew, J. Moreland, J. Kitching, and L. Hollberg, "Atomic vapor cells for miniature frequency references," in *Proceedings of the 2003 IEEE International Frequency Control Symposium and PDA Exhibition Jointly with the 17th European Frequency and Time Forum* (IEEE, 2003), pp. 31–32.
13. E. Arimondo, "Coherent population trapping in laser spectroscopy," in *Progress in Optics*, Vol. XXXV, E. Wolf, ed. (Elsevier, 1996), pp. 257–354.
14. S. Knappe, P. D. D. Schwindt, V. Shah, L. Hollberg, J. Kitching, L. Liew, and J. Moreland, "A chip-scale atomic clock based on Rb-87 with improved frequency stability," *Opt. Express* **13**, 1249–1253 (2005).
15. J. Vanier, A. Godone, and F. Levi, "Coherent microwave emission in coherent population trapping: origin of the energy and of the quadratic light shift," in *Proceedings of the 1999 Joint Meeting of the European Frequency and Time Forum and the IEEE International Frequency Control Symposium* (IEEE, 1999), pp. 96–99.
16. M. Zhu and L. Cutler, "Theoretical and experimental study of light shift in CPT-based Rb vapor cell frequency standard," in *Proceedings of the 32th Precise Time and Time Interval (PTTI) Systems and Applications Meeting* (U.S. Naval Observatory, 2000), pp. 311–324.
17. M. Zhu and S. Cutler, "Coherent population trapping-based frequency standard having a reduced magnitude of total A.C. Stark shift," U.S. patent 6,201,821 (March 13, 2001).
18. S. Kobayashi, Y. Yamamoto, Y. Ito, and T. Kimura, "Direct modulation in Al-GaAs semiconductor lasers," *IEEE J. Quantum Electron.* **18**, 582–595 (1982).
19. P. N. Melentiev, M. V. Subbotin, and V. I. Balykin, "Simple and effective modulation of diode lasers," *Laser Phys.* **11**, 891–896 (2001).
20. C. H. Henry, "Theory of the linewidth of semiconductor-lasers," *IEEE J. Quantum Electron.* **18**, 259–264 (1982).
21. K. Vahala and A. Yariv, "Semiclassical theory of noise in semiconductor-lasers part 1," *IEEE J. Quantum Electron.* **19**, 1096–1101 (1983).
22. H. P. Zappe, "Vertical cavity lasers for atomic time standards," in *Proceedings of the 31st Precise Time and Time Interval (PTTI) Systems and Applications Meeting* (U.S. Naval Observatory, 1999).
23. H. J. Unold, M. Grabherr, F. Eberhard, F. Mederer, R. Jäger, M. Riedl, and K. J. Ebeling, "An increased-area oxidized single-fundamental mode VCSEL with a self-aligned shallow etched surface relief," *Electron. Lett.* **35**, 1340–1341 (1999).
24. J. Vanier, "Coherent population trapping for the realization of a small, stable atomic clock," in *Proceedings of the 2002 IEEE International Frequency Control Symposium and PDA Exhibition* (IEEE, 2002), p. 424.
25. R. Lutwak, D. Emmons, W. Riley, and R. M. Garvey, "The chip-scale atomic clock-coherent population trapping vs. conventional interrogation," in *Proceedings of the 34th Precise Time and Time Interval (PTTI) Systems and Applications Meeting* (U.S. Naval Observatory, 2002).